Features of the Magnetic and Magnetoelectric Properties of HoAl₃(BO₃)₄

$$\text{Features of the Magnetic and Magnetoelectric Properties of HoAl}_3(\text{BO}_3)_4$$

A. I. Begunov[a], A. A. Demidov[a, *], I. A. Gudim[b], and E. V. Eremin[b]

[a] Bryansk State Technical University, Bryansk, 241035 Russia

* e-mail: demandr@yandex.ru

[b] Kirensky Institute of Physics, Siberian Branch, Russian Academy of Sciences, Krasnoyarsk, 660038 Russia

Received March 14, 2013; in final form, April 8, 2013

The main features of the magnetic and record magnetoelectric properties of a $HoAl_3(BO_3)_4$ aluminoborate single crystal have been studied experimentally and theoretically. It has been found that the electric polarization that was previously detected in $HoAl_3(BO_3)_4$ and is record for multiferroics is significantly larger, $\Delta P_{ba}(B_a) \approx -5240\ \mu C/m^2$, with an increase in the magnetic field to 9 T at $T = 5$ K. The measured magnetic properties and revealed features have been interpreted within a united theoretical approach based on the molecular field approximation and on calculations in the crystal field model for a rare-earth ion. The experimental temperature (from 3 to 300 K) and field (up to 9 T) dependences of the magnetization have been described. The parameters of the crystal field of trigonal symmetry for a Ho^{3+} ion in $HoAl_3(BO_3)_4$ have been determined from the interpretation of the experimental data.

DOI: 10.1134/S002136401309004X

INTRODUCTION

Trigonal rare-earth borates $RM_3(BO_3)_4$ (where R = Y, La−Lu; M = Fe, Al, Cr) have been intensively studied in recent years by many Russian and foreign groups (see, e.g., [1−6]). It has already been established that many ferroborates $RFe_3(BO_3)_4$ belong to a new class of multiferroics in which magnetic, electric, and elastic order parameters coexist (see [1, 2, 6−9] and review [10]). Interest in ferroborates is growing every year. The giant magnetodielectric effect has recently been detected in $SmFe_3(BO_3)_4$ [8].

Rare-earth aluminoborates $RAl_3(BO_3)_4$ combine good luminescent properties and pronounced nonlinear optical properties. They belong to new-generation materials for lasers. In particular, ultrashort (femtosecond) laser pulses were obtained on $Yb:YAl_3(BO_3)_4$ crystals [11]. A large magnetoelectric effect comparable with those observed in isostructural ferroborates $RFe_3(BO_3)_4$ was detected in $TmAl_3(BO_3)_4$ [12].

The recent detection of the giant magnetoelectric effect in aluminoborate $HoAl_3(BO_3)_4$ [13] belongs to the most important results for borates $RM_3(BO_3)_4$. The electric polarization in $HoAl_3(BO_3)_4$ in a field of 7 T at $T = 3$ K is $\Delta P_{ab}(B_b) \approx 3600\ \mu C/m^2$ [13, 14], which is maximal for multiferroics and is several times larger than the known maximum polarizations, including those in ferroborates (~500 $\mu C/m^2$ in $SmFe_3(BO_3)_4$ [7] and about 300 $\mu C/m^2$ in $NdFe_3(BO_3)_4$ [2]).

In this work, the main features of the magnetic and record magnetoelectric properties of $HoAl_3(BO_3)_4$ are studied experimentally and theoretically, the measured magnetic characteristics are compared to the calculations within the united theoretical approach, and the parameters of the compound are determined.

EXPERIMENT

$HoAl_3(BO_3)_4$ single crystals were grown from solution−melts based on bismuth trimolybdate and lithium molybdate [15] 90 wt % [$Bi_2Mo_3O_{12}$ + 1.5B_2O_3 + 0.4Li_2MoO_4] + 10 wt % $HoAl_3(BO_3)_4$ using the technology described in detail in [16]. The grown crystals with sizes of 5−8 mm had a small triangular face {0001} of a pinacoid that was perpendicular to the C_3 axis. The fabricated samples had a high optical quality and did not contain visible defects. The magnetic properties of the samples were examined with a vibration magnetometer (Quantum Design) in the temperature range of 3−300 K in magnetic fields up to 9 T. The magnetoelectric studies were performed so that a charge between two contacts (deposited by epoxy with a conducting filler) applied to opposite sides of a plane-parallel plate was measured with a Keithley 6517B electrometer. The temperature and magnetic field were controlled using a PPMS-9 physical property measurement system (Quantum Design).

METHOD OF CALCULATIONS

Experience and successful investigations of isostructural ferroborates $RFe_3(BO_3)_4$ with the Ho^{3+} ion [17, 18] and other rare-earth ions R (see, e.g., [4, 19]), as well as of paramagnetic rare-earth zircons RXO_4 (X = P, V) [20] and perovskite $HoBa_2Cu_3O_{7-x}$ [21, 22], were used in the calculations. The theoretical approach is based on the crystal field model for a rare-earth ion and on the molecular field approximation.

To calculate the magnetic characteristics of the $HoAl_3(BO_3)_4$ paramagnetic compound and Zeeman effect, we used the Hamiltonian $\mathcal{H}$ including the crystal field Hamiltonian $\mathcal{H}_{CF}$, Zeeman term $\mathcal{H}_Z$, and hyperfine interaction Hamiltonian $\mathcal{H}_{HF}$:

$$\mathcal{H} = \mathcal{H}_{CF} + \mathcal{H}_Z + \mathcal{H}_{HF}, \tag{1}$$

$$\begin{aligned}\mathcal{H}_{CF} &= B_0^2 C_0^2 + B_0^4 C_0^4 + B_3^4(C_{-3}^4 - C_3^4) + B_0^6 C_0^6 \\ &+ B_3^6(C_{-3}^6 - C_3^6) + B_6^6(C_{-6}^6 + C_6^6),\end{aligned} \tag{2}$$

$$\mathcal{H}_Z = -g_J \mu_B \mathbf{BJ}, \tag{3}$$

$$\mathcal{H}_{HF} = A_J \mathbf{JI}. \tag{4}$$

Here, B_q^k are the parameters of the crystal field for the D_3 symmetry, C_q^k are the irreducible tensor operators, g_J is the Landé factor, $\mathbf{J}$ is the angular momentum operator of the rare-earth ion, A_J is the hyperfine coupling constant, and $\mathbf{I}$ is the nuclear spin operator. The hyperfine interaction Hamiltonian was taken in the form of Eq. (4) as for a free ion with $A_J \approx 0.027$ cm^{-1} [23].

The magnetization of the $HoAl_3(BO_3)_4$ paramagnetic compound in the external field $\mathbf{B}$ is

$$\mathbf{M} = g_J \mu_B \langle \mathbf{J} \rangle. \tag{5}$$

The magnetic characteristics were calculated from the spectrum and wavefunctions of the Ho^{3+} ion, which were calculated through the numerical diagonalization of the Hamiltonian $\mathcal{H}$ for each set of B and T values.

The contribution of the holmium subsystem to the specific heat of $HoAl_3(BO_3)_4$ was calculated by the usual quantum-mechanical formula

$$C_{Ho} = k_B \frac{\langle E^2 \rangle - \langle E \rangle^2}{(k_B T)^2}. \tag{6}$$

The thermal means $\langle E^2 \rangle$ and $\langle E \rangle^2$ were calculated for the spectrum of the Ho^{3+} ion formed by the crystal field and external magnetic field.

RESULTS AND DISCUSSION

We begin the description of the magnetic properties of $HoAl_3(BO_3)_4$ with the determination of the parameters of the crystal field B_q^k because the crystal field, which forms the electronic structure of the rare-earth ion (its spectrum and wavefunctions), is responsible for the anisotropy of the magnetic properties of rare-earth aluminoborates.

Neogy et al. [24] measured the magnetic susceptibility $\chi_{c, \perp c}(T)$ of $HoAl_3(BO_3)_4$ at 12 temperatures in the range $T = 14.5-300$ K with a large temperature step. Then, Neogy et al. [24] attempted to determine the parameters of the crystal field for the Ho^{3+} ion in $HoAl_3(BO_3)_4$ using the description of measured $\chi_{c, \perp c}(T)$ points as the only criterion of the correctness of the determination of B_q^k. The experience of investigations of rare-earth compounds shows that a reliable set of parameters of the crystal field usually cannot be determined using only the susceptibility curves (the more so, without the actual low-temperature section). The lower part of the fundamental multiplet for holmium compounds is often characterized by the presence of several close levels. For this reason, one can find several sets of parameters of the crystal field that describe well the anisotropy of susceptibility curves, but significantly differ in the values, and determine different structures of Stark energy levels and different wavefunctions. Thus, the set of parameters of the crystal field found in [24] cannot be considered as reliable. The resulting theoretical curves $\chi_{c, \perp c}(T)$, the scheme of Stark levels, and the calculation of thermal and hyperfine properties should be revised. The intersection of $\chi_c(T)$ and $\chi_{\perp c}(T)$ near 2 K predicted in [24] is not confirmed experimentally, because the $\chi_{c, \perp c}(T)$ curves measured in our work down to 3 K do not exhibit a tendency to possible intersection even at lower temperatures. No intersection of the $\chi_{c, \perp}(T)$ curves measured down to a lower temperature of 2 K was observed in [13]. It was also established that the magnetization curves $M_{c, \perp c}(B)$ calculated with the parameters of the crystal field from [24] differ significantly from the experimental curves measured in our work.

The parameters of the crystal field were sought taking into account the known spectroscopic information from [25]. Although aluminoborate $YAl_3(BO_3)_4:Ho^{3+}$, rather than $HoAl_3(BO_3)_4$, was studied in [25], the level schemes (the order of doublets and singlets and their number) for these two compounds should hardly be strongly different. However, differences in particular splittings between levels are allowable. The calculation with the parameters of the crystal field for $YAl_3(BO_3)_4:Ho^{3+}$ from [25] and the subsequent comparison with the magnetic characteristics measured in this work show that the theoretical $M_{c, \perp c}(B)$ curves are slightly above the experimental curves. The intersec-
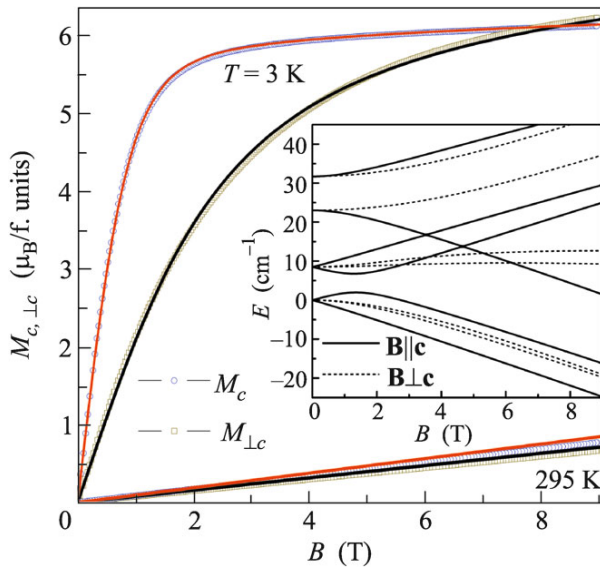
Fig. 1. (Points) Experimental and (lines) theoretical magnetization curves of $HoAl_3(BO_3)_4$ for $\mathbf{B} \parallel \mathbf{c}$ and $\mathbf{B} \perp \mathbf{c}$ at $T = 3$ and 295 K. The inset shows the Zeeman effect at $T = 3$ K. Six lower energy levels of the ground multiplet of the Ho^{3+} for (solid lines) $\mathbf{B} \parallel \mathbf{c}$ and (dashed lines) $\mathbf{B} \perp \mathbf{c}$ are shown.

tion of $M_{c, \perp c}(B)$ occurs near 6 T (near 8 T for the experimental curve). However, the theoretical curves qualitatively describe the experiment. The $M_{c, \perp c}(T)$ curves calculated with the parameters of the crystal field from [25] are similarly above the experimental curves. The scheme of the energy levels determined in [25] for the ground multiplet of the Ho^{3+} ion in $YAl_3(BO_3)_4$:Ho^{3+} is exactly reproduced with noncritical differences in particular splittings between levels with the set of parameters of the crystal field for the Ho^{3+} ion in $HoAl_3(BO_3)_4$ found in our work.

We began the minimization procedure of the corresponding objective function with the initial values of the parameters of the crystal field for $HoFe_3(BO_3)_4$ [17, 18], $YAl_3(BO_3)_4$:Ho^{3+} [25], and $NdAl_3(BO_3)_4$ [26]. To determine the parameters of the crystal field, we used the experimental temperature dependences of the magnetization $M_{c, \perp c}(T)$ of $HoAl_3(BO_3)_4$ in the range from 3 to 300 K at $B = 0.1$ and 3 T. As should be expected, several sets of parameters of the crystal field describe well the anisotropy of $M_{c, \perp c}(T)$ curves. Their main difference is that they give different distances between lower energy levels of the Ho^{3+} ion. Then, information on the experimental magnetization curves $M_{c, \perp c}(B)$ at $T = 3$ K in fields up to 9 T was additionally introduced in the objective function. This made it possible to reject several found sets of parameters of the crystal field.

As a result, using the listed criteria for the description of the $M_{c, \perp c}(T)$ and $M_{c, \perp c}(B)$ curves and existing

information on the structure of the ground multiplet [25], from all parameters B_q^k of the crystal field found at the initial stage, we chose the following set that provides the best description of the experimental data for $HoAl_3(BO_3)_4$ (in inverse centimeters):

$$B_0^2 = 670, \quad B_0^4 = -1693, \quad B_3^4 = -364,$$
$$B_0^6 = 83, \quad B_3^6 = -414, \quad B_6^6 = -663. \tag{7}$$

These parameters were determined from the calculations on the basis of the ground multiplet. Consequently, they can be treated only as effective parameters applicable for the description of the thermodynamic properties of the compound.

Parameters (7) correspond to the following energies of 17 lower Stark levels of the ground multiplet of the Ho^{3+} ion in $HoAl_3(BO_3)_4$ ($B = 0$, $T = 3$ K): 0, 0, 8.5, 8.5, 23, 31.7, 116, 160, 160, 271, 271, 315, 371, 371, 429, 429, and 453 cm^{-1}. Parameters (7) correspond to the components $g_a = 1.84$ and $g_c = 2.52$ of the ground non-Kramers doublet of the Ho^{3+} ion. The determined energies of lower energies of the ground multiplet of the Ho^{3+} ion are close to energies determined for $T = 9$ K in [25].

According to the experimental and theoretical magnetization curves of $HoAl_3(BO_3)_4$ for $T = 3$ and 295 K shown in Fig. 1, the $M_{c, \perp c}(B)$ curves for $T = 3$ K increase at different rates with an increase in the field, demonstrating significant anisotropy. The evolution of the $M_{c, \perp c}(B)$ curves with an increase in the temperature occurs owing to a decrease in the magnetic moment of the holmium subsystem. The calculation with parameters (7) throughout the entire field range for $T = 3$ and 295 K provides a good description of the behavior of the corresponding experimental curves. The Zeeman effect corresponding to the $M_{c, \perp c}(B)$ curves calculated for $T = 3$ K is shown in the inset in Fig. 1. It can be seen that the splitting of the energy levels of the Ho^{3+} ion for $\mathbf{B} \parallel \mathbf{c}$ is larger than that for $\mathbf{B} \perp \mathbf{c}$.

We also calculated the Zeeman effect in strong fields (up to 200 T) at $\mathbf{B} \parallel \mathbf{c}$ and $\mathbf{B} \perp \mathbf{c}$ in order to analyze possible effects associated with the interaction of energy levels of the Ho^{3+} ion in the magnetic field (crossover), which provide valuable information on the crystal field. Crossovers are observed for almost all rare-earth elements R in paramagnetic compounds RXO_4 (X = P, V) with the zircon structure and are accompanied by pronounced magnetic anomalies on magnetic characteristics (see, e.g., [20−22]). Similar effects in intermediate and strong magnetic fields are expected in aluminoborates $RAl_3(BO_3)_4$. The calculations show that the crossover occurs in $HoAl_3(BO_3)_4$ for $\mathbf{B} \parallel \mathbf{c}$ and $T = 3$ K near 75 T and results in a small jump (~0.5 μ_B) on the $M_c(B)$ curve and the corresponding maximum on the differential magnetic sus-

ceptibility dM_c/dB. The crossover on $M_a(B)$ for **B ∥ a** and $T = 1.5$ K is possible in lower fields near 11 T with a jump of about $0.7\mu_B$. The calculations with various parameters of the crystal field show that fields in which crossovers occur depend strongly on particular parameters of the crystal field and can be indicators for their more accurate determination.

Figure 2 shows the experimental and theoretical temperature dependences of the magnetization $M_{c, \perp c}(T)$ at $B = 0.1$ T. It can be seen that the calculations with parameters (7) describe well the experimental $M_{c, \perp c}(T)$ curves. It is interesting that the theoretical $M_{\perp c}(T)$ curve (the inset in Fig. 2) at low temperatures tends to a constant of $M_{\perp c} = 0.226$ μ_B/f.u. at $B = 0.1$ T. We also calculated the magnetic susceptibility $\chi_{c, \perp c}(T)$ of $HoAl_3(BO_3)_4$ at $B = 0.1$ T by the known Van Vleck formula. This calculation gave results similar to the theoretical $M_{c, \perp c}(T)$ curves at $B = 0.1$ T. The analysis of the low-temperature parts of the experimental $M_{\perp c}(T)$ curves (measured down to 3 K) and $\chi_c(T)$ (measured down to 2 K in [13]) cannot exclude that the experimental $M_{\perp c}(T)$ and $\chi_c(T)$ curves at $T < 2$ K tend to constants, as was predicted in the calculations. The $\chi_{x, z}(T)$ curves for $TmAl_3(BO_3)_4$ and $TbAl_3(BO_3)_4$ at low temperatures tend to constants [14].

We tried to obtain an increase in the theoretical $M_{\perp c}(T)$ curve with a decrease in the temperature at $T < 2$ K. The effect of the hyperfine interaction on the magnetic characteristics of rare-earth compounds with Van Vleck ions (Pr^{3+}, Tb^{3+}, Ho^{3+}, Tm^{3+}) increases at low temperatures and can be determining. In particular, it was shown in [21, 22] that the hyperfine interaction is significant for the description of phase diagrams in $HoBa_2Cu_3O_{7-x}$ at $T \approx 1$ K owing to the effect on the energy spectrum of the Ho^{3+} ion. The Hamiltonian of the hyperfine interaction was taken in the form of Eq. (4), as for a free ion. The hyperfine interaction splits each of the energy levels of the Ho^{3+} ion into eight components ($I = 7/2$ for ^{165}Ho). The calculations including the hyperfine interaction (green line $M_{\perp c}(T)$ in the inset in Fig. 2) show that a small increase in $M_{\perp c}(T)$ is possible only at $T < 1.7$ K. Thus, the inclusion of the hyperfine interaction in the form of Eq. (4) did not lead to significant changes in the low-temperature part of the theoretical $M_{c, \perp c}(T)$ curves and generally confirmed the predicted shape of the $M_{\perp c}(T)$ curve at $T < 2$ K.

We performed the calculations taking into account the nuclear Zeeman interaction ($\mathcal{H}_z = -\gamma_I \hbar \mathbf{BI}$). In this case, Hamiltonian (1) was supplemented by the effective nuclear spin Hamiltonian of the hyperfine interaction (see, e.g., [27]). The parameters of the hyperfine-interaction spin Hamiltonian for $HoAl_3(BO_3)_4$ are unknown. For this reason, the calculation was performed with the parameters for $HoVO_4$ [27] ($\gamma_\perp/2\pi = 1527$ MHz/T and $\gamma_\parallel/2\pi = 15$ MHz/T).
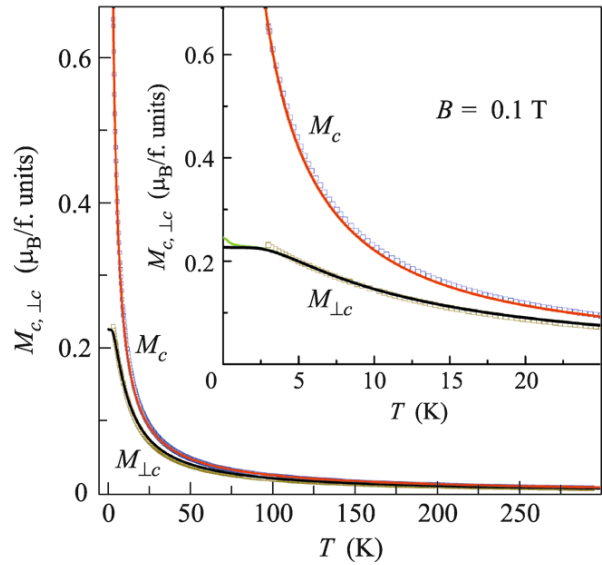

Fig. 2. (Color online) (Points) Experimental and (lines) theoretical temperature dependences of the magnetization $M_{c, \perp c}(T)$ of $HoAl_3(BO_3)_4$ at $B = 0.1$ T. The inset shows the low-temperature region of $M_{c, \perp c}(T)$ (the green line is the calculation including the hyperfine interaction).

It was found that the inclusion of the nuclear Zeeman interaction in the calculation of $M_{c, \perp c}(T)$ for the field $B = 0.1$ T also does not lead to significant changes: the theoretical $M_{\perp c}(T)$ curve at $T < 2$ K tends to a constant. The calculations with various parameters of the spin Hamiltonian show that $M_{\perp c}(T)$ begins to increase at $T < 2$ K if the parameter $\gamma_\perp/2\pi$ is increased by 40%. As a result, the possible experimental detection of a further increase in $M_{\perp c}(T)$ at $T < 2$ K will promote the determination of the parameters of the hyperfine interaction for $HoAl_3(BO_3)_4$ and the absence of an increase in $M_{\perp c}(T)$ will confirm our calculation.

The experimental and theoretical $M_{c, \perp c}(T)$ curves presented in Fig. 3 for $B = 3$, 6, and 9 T show that the anisotropy of the $M_{c, \perp c}(T)$ curves at low temperatures (inset in Fig. 3) changes differently for different B values (see also $M_{c, \perp c}(T)$ at $B = 0.1$ T in Fig. 2) and is quite well described throughout the entire temperature range. At $T = 3$ K, $M_c/M_{\perp c} = 2.83$, 1.32, 1.05, and 0.98 for $B = 0.1$, 3, 6, and 9 T, respectively. At $T = 15$ K, $M_c/M_{\perp c} = 1.43$, 1.31, 1.14, and 1.04 for $B = 0.1$, 3, 6, and 9 T, respectively.

The experimental temperature dependences of the difference $M_c - M_{\perp c}$ for $B = 0.1$, 3, 6, and 9 T shown in Fig. 4 make it possible to estimate how the temperature dependence of the magnetization anisotropy changes with an increase in the field. It can be seen that $M_c > M_{\perp c}$ for all measured B values, except for a small low-temperature section at $B = 9$ T. The difference $M_c - M_{\perp c}$ at high temperatures ($T > 50$ K) increases with the field B. The discussed curves at $T <$
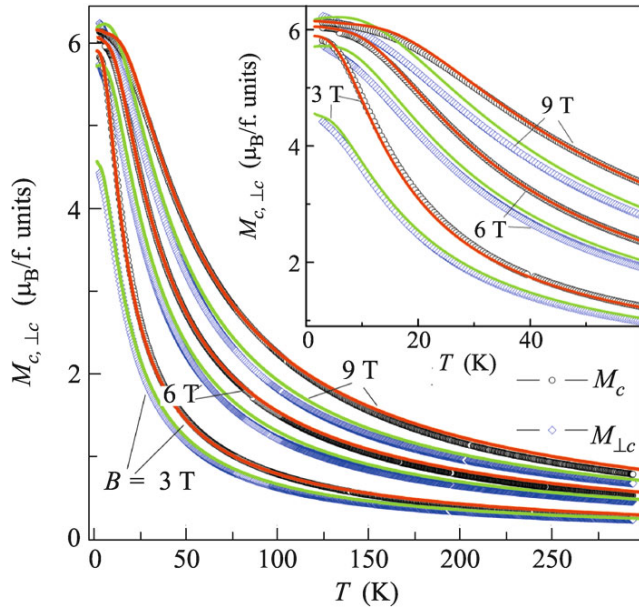
Fig. 3. (Color online) (Points) Experimental and (lines) theoretical temperature dependences of the magnetization $M_{c, \perp c}(T)$ of HoAl$_3$(BO$_3$)$_4$ at $B = 3$, 6, and 9 T. The inset shows the low-temperature region of $M_{c, \perp c}(T)$. The red and green lines correspond to $M_c(T)$ and $M_{\perp c}(T)$.
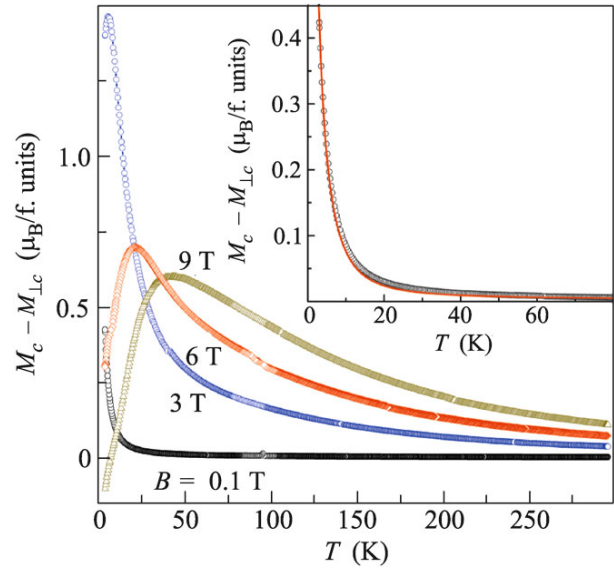

Fig. 4. Experimental temperature dependences of the difference $M_c - M_{\perp c}$ of HoAl$_3$(BO$_3$)$_4$ at $B = 0.1$, 3, 6, and 9 T. The inset shows the low-temperature region of the experimental and theoretical temperature dependences of the difference $M_c - M_{\perp c}$ at $B = 0.1$ T.

50 K exhibit a more complex dependence. For example, all curves at $B > 0.1$ T have a low-temperature section (expanding with an increase in B) where the anisotropy of the magnetization curves increases with the temperature.

No experimental data for the specific heat of HoAl$_3$(BO$_3$)$_4$ have been reported. Using the parameters of the crystal field determined when describing the magnetic characteristics, we calculated the contribution of the holmium subsystem to the specific heat of HoAl$_3$(BO$_3$)$_4$ (Fig. 5) (solid lines) with and (dashed lines) without the inclusion of the hyperfine interaction. The wide peak on the $C_{Ho}(T)$ curve at $B = 0$ near 6.2 K calculated disregarding the hyperfine interaction (black dashed line) is the Schottky anomaly. This peak is attributed to the redistribution of the populations of two lower levels of the ground doublet of the Ho^{3+} ion. The hyperfine interaction in the form of Eq. (4) splits the ground doublet of the Ho^{3+} ion (each level of the doublet is split into eight components) and, as a result, an additional sharp peak (Schottky anomaly) appears on $C_{Ho}(T)$ near 0.18 K ($B = 0$).

Figure 5 shows the $C_{Ho}(T)$ curves in the field **B** ∥ **c** for $B = 1$, 3, and 6 T and (inset) $B = 0.1$, 0.3, and 0.5 T. It can be seen that the calculation predicts not only the shift of the wide peak with an increase in the field **B** ∥ **c** toward higher temperatures but also the appearance of several additional anomalies (a sharp peak in the range of 0.2–0.3 K and a smooth peak at 0.6–4.8 K depending on the applied field B).
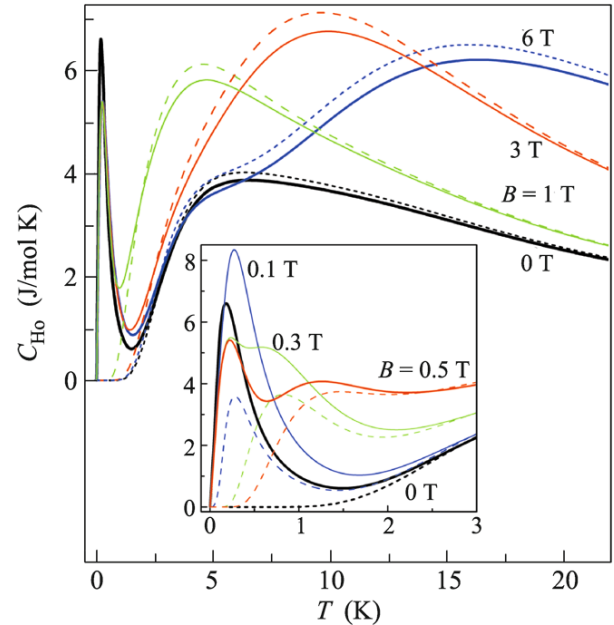

Fig. 5. Theoretical contribution of the Ho subsystem to the specific heat of HoAl$_3$(BO$_3$)$_4$ (solid lines) with and (dashed lines) without the inclusion of the hyperfine interaction for various B values at **B** ∥ **c**. The inset shows the low-temperature region of the calculated contribution for low B values.

Figure 6 shows the field dependences of the transverse, $\Delta P_{ba}(B_a)$ and $\Delta P_{bc}(B_c)$, and longitudinal, $\Delta P_{bb}(B_b)$, electric polarization of $HoAl_3(BO_3)_4$ for various temperatures. The strong anisotropy of $\Delta P_b(B)$ depending on the direction of the magnetic field is clearly seen in the inset in Fig. 6a. An increase in the field is accompanied by a noticeable increase in the electric polarization caused by the electronic structure of the Ho^{3+} ion and its spectrum in the trigonal crystal field of aluminoborate $HoAl_3(BO_3)_4$. The observed longitudinal polarization at $T = 5$ K in the field $B = 9$ T reaches $\Delta P_{ba}(B_a) \approx -5240$ $\mu C/m^2$, which is much larger in absolute value than the record value $\Delta P_{ab}(B_b) \approx -3600$ $\mu C/m^2$ for multiferroics found at 3 K in a field of 7 T [13, 14]. It is interesting that our preliminary investigations of similar dependences of the electric polarization of new aluminoborate $HoAl_{2.5}Ga_{0.5}(BO_3)_4$ show that $\Delta P(B)$ for this aluminoborate (at the respective T and B values) is much smaller than that for $HoAl_3(BO_3)_4$. This is likely due to the effect of the changed crystal field and, as a result, to the changed structure (splittings between the energy levels) of the ground multiplet of the Ho^{3+} ion in $HoAl_{2.5}Ga_{0.5}(BO_3)_4$.

According to Fig. 6, the behavior of all components of the electric polarization as quadratic functions of the magnetic field does not induce any phase transitions that were detected on similar dependences in isostructural ferroborates [1, 2, 6–10]. The observed temperature dependence of $\Delta P(B)$ in $HoAl_3(BO_3)_4$ is due to the increasing temperature dependence of the population of excited states of the Ho^{3+} ion. It can be seen that the field dependences $\Delta P(B)$ in $HoAl_3(BO_3)_4$ decrease monotonically with an increase in the temperature without jumps as, e.g., in $HoFe_3(BO_3)_4$ at $T_{SR} \approx 5$ K [28]. This difference in the behavior of the $\Delta P(B)$ curves is due not only to the effect if the f–d interaction in $HoFe_3(BO_3)_4$ but also to various features of the electronic structures of the Ho^{3+} ion in $HoAl_3(BO_3)_4$ and $HoFe_3(BO_3)_4$. The Stark levels of the ground multiplet of the Ho^{3+} ion in $HoFe_3(BO_3)_4$ at low temperatures and $B = 0$ are split into the singlets of 0, 7.7, 10.6, 30.3, 36, 64.3, and 198 cm^{-1} [17]. Two non-Kramers doubles are observed in the lower part of the multiplet of the Ho^{3+} ion in $HoAl_3(BO_3)_4$ (see above).

The symmetry analysis in [2] predicted the field-quadratic contributions to the polarization and a change in its sign upon a change in the direction of the field by 90°. This prediction is experimentally confirmed for $HoAl_3(BO_3)_4$ upon a change in the direction of the field from **B** ‖ **a** (Fig. 6a) to **B** ‖ **b** (Fig. 6b). Since a similar feature was previously observed for ferroborates $HoFe_3(BO_3)_4$ [28], $SmFe_3(BO_3)_4$ [7], and
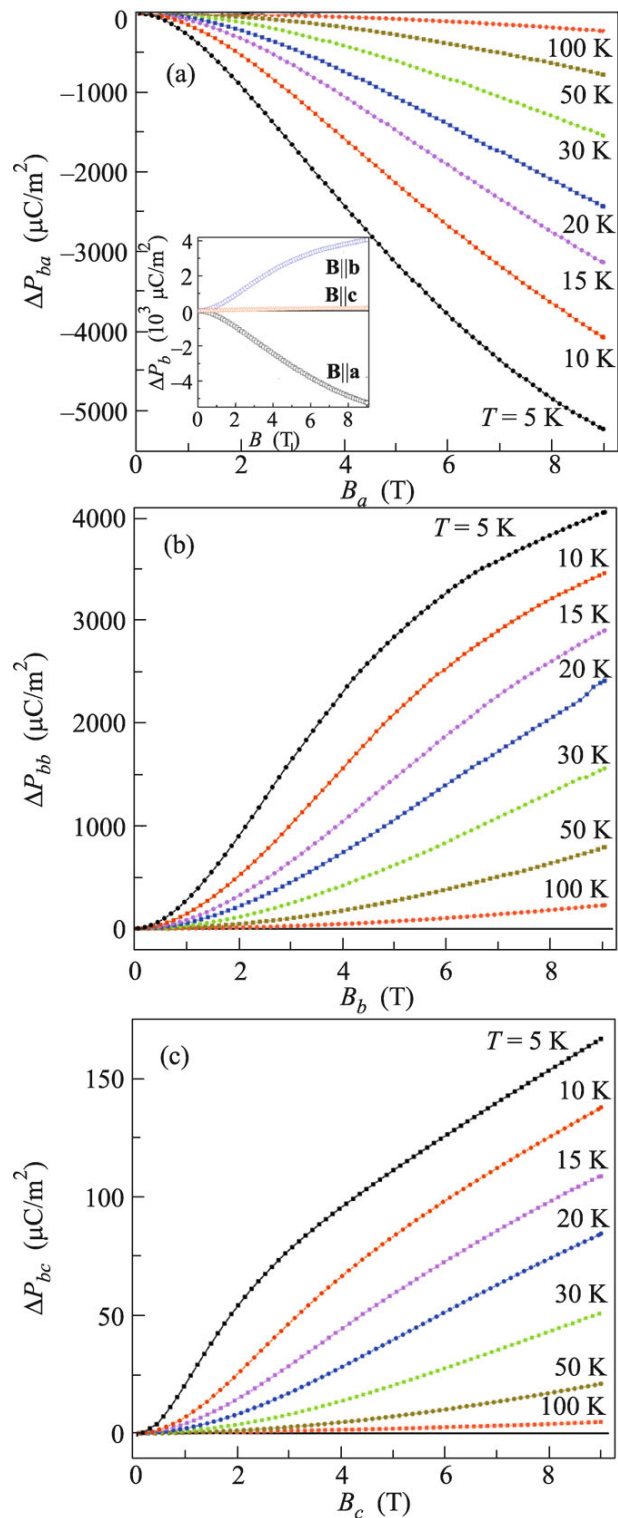

Fig. 6. Experimental field dependences of the (a, c) transverse and (b) longitudinal electric polarization of $HoAl_3(BO_3)_4$ for various temperatures. The inset shows the $\Delta P_b(B_{abc})$ at $T = 5$ K.

$NdFe_3(BO_3)_4$ [2], we can conclude that the role of the rare-earth subsystem in the magnetoelectric properties of rare-earth borates $RM_3(BO_3)_4$ is decisive.

CONCLUSIONS

To summarize, we have found that the giant magnetoelectric effect occurs in a $HoAl_3(BO_3)_4$ single crystal. The measurements for strong fields indicate its record value. The magnetic properties of $HoAl_3(BO_3)_4$ have been studied experimentally and theoretically. The theoretical results are in agreement with the experimental data for all sets of measured magnetic characteristics. The parameters of the crystal field in $HoAl_3(BO_3)_4$ have been determined. Analyzing the role of the hyperfine interaction, we have determined its effect on the magnetic characteristics and predicted possible anomalies on the experimental dependences of the specific heat of $HoAl_3(BO_3)_4$.

Further investigation of $HoAl_3(BO_3)_4$ is necessary. The theoretical explanation and description of the detected giant magnetoelectric effect and its features are certainly of interest. We are going to describe not only the magnetic but also the magnetoelectric characteristics of $HoAl_3(BO_3)_4$ within a united approach based on the results reported in [9, 29].

REFERENCES

1. A. K. Zvezdin, S. S. Krotov, A. M. Kadomtseva, et al., JETP Lett. **81**, 272 (2005).

2. A. K. Zvezdin, G. P. Vorob'ev, A. M. Kadomtseva, et al., JETP Lett. **83**, 509 (2006).

3. A. M. Kuz'menko, A. A. Mukhin, V. Yu. Ivanov, et al., JETP Lett. **94**, 275 (2011).

4. E. A. Popova, D. V. Volkov, A. N. Vasiliev, et al., Phys. Rev. B **75**, 224413 (2007).

5. E. A. Popova, N. I. Leonyuk, M. N. Popova, et al., Phys. Rev. B **75**, 054446 (2007).

6. R. P. Chaudhury, F. Yen, B. Lorenz, et al., Phys. Rev. B **80**, 104424 (2009).

7. Yu. F. Popov, A. P. Pyatakov, A. M. Kadomtseva, et al., J. Exp. Theor. Phys. **111**, 199 (2010).

8. A. A. Mukhin, G. P. Vorob'ev, V. Yu. Ivanov, et al., JETP Lett. **93**, 294 (2011).

9. A. I. Popov, D. I. Plokhov, and A. K. Zvezdin, Phys. Rev. B **87**, 024413 (2013).

10. A. M. Kadomtseva, Yu. F. Popov, G. P. Vorob'ev, et al., J. Low Temp. Phys. **36**, 532 (2010).

11. N. I. Leonyuk, V. V. Maltsev, E. A. Volkova, et al., Opt. Mater. **30**, 161 (2007).

12. R. P. Chaudhury, B. Lorenz, Y. Y. Sun, et al., Phys. Rev. B **81**, 220402 (2010).

13. K.-C. Liang, R. P. Chaudhury, B. Lorenz, et al., Phys. Rev. B **83**, 180417(R) (2011).

14. K.-C. Liang, R. P. Chaudhury, B. Lorenz, et al., J. Phys.: Conf. Ser. **400**, 032046 (2012).

15. L. N. Bezmaternykh, V. L. Temerov, I. A. Gudim, et al., Crystallogr. Rep. **50**, 97 (2005).

16. V. L. Temerov, A. E. Sokolov, A. L. Sukhachev, et al., Crystallogr. Rep. **53**, 1157 (2008).

17. A. A. Demidov and D. V. Volkov, Phys. Solid State **53**, 985 (2011).

18. A. A. Demidov, I. A. Gudim, and E. V. Eremin, J. Exp. Theor. Phys. **115**, 815 (2012).

19. A. A. Demidov, I. A. Gudim, and E. V. Eremin, J. Exp. Theor. Phys. **114**, 259 (2012).

20. A. A. Demidov, Z. A. Kazei, N. P. Kolmakova, et al., Phys. Rev. B **70**, 134432 (2004).

21. Z. A. Kazei, A. A. Demidov, and N. P. Kolmakova, J. Magn. Magn. Mater. **258–259**, 590 (2003).

22. A. A. Demidov, Extended Abstract of Candidate's Dissertation (Moscow State Univ., Moscow, 2004).

23. A. Abraham and B. Bleaney, *Electron Paramagnetic Resonance of Transition Ions* (Clarendon, Oxford, 1970; Mir, Moscow, 1974).

24. D. Neogy, K. N. Chattopadhyay, P. K. Chakrabartia, et al., J. Magn. Magn. Mater. **154**, 127 (1996).

25. A. Baraldi, R. Capelletti, M. Mazzera, et al., Phys. Rev. B **76**, 165130 (2007).

26. C. Cascales, C. Zaldo, U. Caldino, et al., J. Phys.: Condens. Matter. **13**, 8071 (2001).

27. B. Bleaney, J. F. Gregg, P. Hansen, et al., Proc. R. Soc. London **416**, 63 (1988).

28. A. M. Kadomtseva, G. P. Vorob'ev, Yu. F. Popov, et al., J. Exp. Theor. Phys. **114**, 810 (2012).

29. A. A. Mukhin, V. Yu. Ivanov, A. M. Kuz'menko, et al., in *Proceedings of the 36th Workshop on Low Temperature Physics NT-36* (St. Petersburg, 2012), p. 162.

Translated by R. Tyapaev